Application of a Packaged Fiber Bragg Grating Sensor to Outdoor Optical Fiber Cabinets for Environmental Monitoring

Wen-Ping Chen, Fu-Hung Shih, Po-Jun Tseng, Chih-Hsien Shao, and Chia-Chin Chiang

***Abstract*— Outdoor optical fiber cabinets are generally installed along roadsides where environmental conditions, such as sun exposure, rain, and dust, can cause damage to the cabinets. Furthermore, high temperatures and unexpected impacts that cause cabinet deformation may damage the network equipment inside the cabinets, affecting the quality of communications. This paper developed an optical fiber sensing system for real-time monitoring of the temperature variation and external forces exerted on outdoor cabinets using fiber Bragg gratings (FBGs). This FBG sensing system was established in the network management center, and was linked to the outdoor cabinets at the remote end through optical fibers in order to monitor the impacts and temperature changes of the cabinets. Experimental results revealed that exerting an external impact force of 297 N on an outdoor cabinet severely dented the impacted cabinet surface. When the monitoring system detects external impacts exceeding 297 N or cabinet temperatures greater than 65 °C, the network management center can then immediately send maintenance personnel to check for any network impairments.**

***Index Terms*— Fiber Bragg grating, outdoor cabinet, optical fiber sensor.**

I. Introduction

BASED on budgetary considerations, telecommunications service providers (TSPs) typically employ copper materials in the last mile of the user-end cable, instead of using optical fibers. Basically, TSPs still require network equipment in outdoor cabinets to link back-end fiber systems with the copper cables of front-end users when providing high-speed Internet service. Thus, the task of maintaining the stability of network equipment in outdoor cabinets so as to offer uninterrupted Internet access on the user-end has become a crucial one for TSPs.

Currently, most outdoor cabinets are installed along roadsides, where environmental conditions are sometimes extremely harsh, including exposure to sun, rain, dust, and the growth of natural organisms, all of which may damage the cabinets. Although issues like airtightness and cooling are considered at the cabinet design stage, the frequent occurrence of cabinet deformations caused by external impacts from unexpected traffic accidents and extremely hot weather conditions can result in a failure to effectively protect the network equipment inside the cabinets, thereby degrading the quality of communications.

Fiber Bragg gratings (FBGs) have been widely adopted for sensing and monitoring in various engineering fields such as aerospace technology [1], the structural monitoring of buildings [2], pressure sensor [3], biosensors [4], railway monitoring systems [5], and overhead transmission line monitoring systems [6]. Moreover, relevant researches have achieved amazing results. Optical fiber sensors possess important properties such as being small in volume, lightweight, low-loss, resistant to corrosion, resistant to electromagnetic interference, and highly sensitive, in addition to having an excellent linear relationship with respect to temperature and strain. Moreover, the use of optical fibers as communication media in monitoring systems allows coverage over areas several kilometers wide, making optical fiber a material well-suited for long-distance monitoring systems.

In 1993, Hill et al. [7] proposed to fabricate optical fiber gratings by using phase masks. In this process, optical fibers are exposed to a UV source, an excimer laser, through phase masks with prescribed wavelengths to create periodic refractive-index variation and generate permanent phase gratings. This method enables the rapid mass production of optical fiber gratings, substantially reducing the cost of manufacturing.

FBG sensors have also been embedded into medical textiles for the monitoring of respiratory movement in magnetic resonance image (MRI), measuring the elongation of the abdominal circumference [4], [8]–[10]. They are also embedded in PVC laminates during the spread-coating process; the resulting structure is a temperature and strain sensitive foil in which the performance is evaluated through the surface structure as well as the optical response [3]. More wearable solutions for monitoring human physical conditions have also been proposed, e.g., for the rehabilitation of patients' hand movements after strokes and for the rehabilitation of knee flexion and extension [4], [5]. FBGs are also used for measuring and monitoring turbine engines [11], inspecting pipeline water leakage [12], measuring high temperatures [13], measuring dynamic and sta-

Manuscript received July 1, 2014; revised August 19, 2014; accepted August 20, 2014. Date of publication August 29, 2014; date of current version November 20, 2014. This work was supported by the National Science Council of Taiwan under Grant NSC-102-2622-E-164-001-CC3 and Grant MOST-103-2221-E-151-009-MY3. The associate editor coordinating the review of this paper and approving it for publication was Dr. Anna G. Mignani.

W.-P. Chen, F.-H. Shih, and P.-J. Tseng are with the Department of Electrical Engineering, National Kaohsiung University of Applied Sciences, Kaohsiung 807, Taiwan.

C.-H. Shao and C.-C. Chiang are with the Department of Mechanical Engineering, National Kaohsiung University of Applied Sciences, Kaohsiung 807, Taiwan (e-mail: ccchiang@kuas.edu.tw).

Color versions of one or more of the figures in this paper are available online at http://ieeexplore.ieee.org.

Digital Object Identifier 10.1109/JSEN.2014.2353040

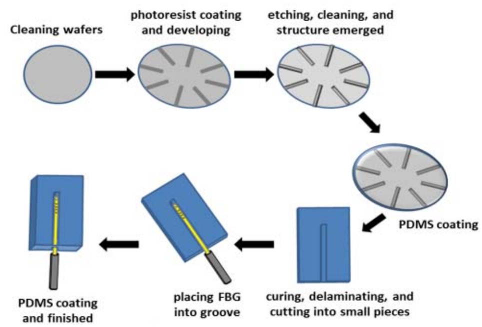

Fig. 1. Manufacturing procedures for PDMS-packaged FBGs.

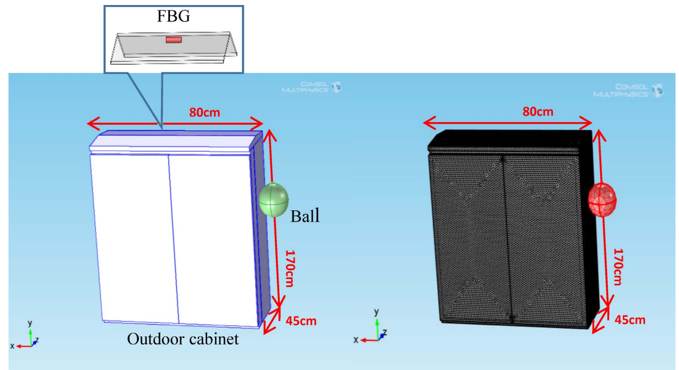

Fig. 2. The modal and mesh of mass impact test of the outdoor optical fiber cabinets.

tic metal cutting forces [14], portably monitoring human body temperatures and the health statuses of patients [15], [16], monitoring energy conversion systems [17], monitoring chemical solvents [18], for intrusion detection in residential security systems [19] and dynamic vehicle loading [14].

However, no previous studies have addressed the application of FBG sensors for monitoring the environments of outdoor cabinets. Therefore, in this study, the linear response to strain and temperature of FBG was adopted to create and test a system for real-time monitoring of the influences of external impacts and temperature increments on outdoor cabinets, including their effects on the quality of network communications.

The equipment inside outdoor cabinets has a high rate of malfunctions, which are mainly caused by damage to circuit boards from high temperatures and the corrosion that arises from cabinet deformation and contamination by dust and microorganisms. High temperatures come from daytime sun exposure as well as the heat generated by the internal network equipment, and these temperatures can be further increased if the air filters in the cabinets become blocked. Because outdoor cabinets are placed on roadsides, they can be deformed by traffic accidents or vandalism. In addition to incurring equipment and property damage to TSPs, these conditions also lead to Internet connection instability at the user end, causing serious customer complaints and damage to company reputations. Consequently, a sensor system for real-time monitoring of the temperature changes and damage to outdoor cabinets could be of great benefit to TSPs and their customers.

II. Experimental Methods

A. Packaged FBG Sensors

In this experiment, polydimethylsiloxane (PDMS) was adopted for the cladding of the FBG sensors. PDMS has favorable features such as superior chemical resistance, high temperature stability, flexibility, and low production costs. Therefore, packaged FBG sensors can be used in many places and can function normally without their optical sensing abilities being influenced by moisture or other chemical properties [20]. Fig. 1 illustrates the manufacturing procedures for packaged FBG sensors used in this study.

B. Fundamentals of Fiber Bragg Grating (FBG)

The FBG sensors employed in the present study were fabricated using a UV excimer laser. Laser light was passed through a phase mask to generate interference and periodic changes in the core refractive index of the photosensitive optical fiber to consequently form optical grating structures. Therefore, this type of grating is also known as reflective fiber grating. The fiber grating used in this study had a grating period of about 1μm. When light emitted from a broadband light source is coupled with the optical fiber, the light reflected by the FBG depends on the variations in the periodic refractive index. The light matching the conditions of the Bragg grating will be reflected, while the rest of the light will be transmitted. The reflected light must have a wavelength satisfying the Bragg condition expressed by the following formula

$$\lambda_B = 2n_{eff}\Lambda \tag{1}$$

in which λ_B represents the Bragg wavelength; n_{eff} denotes the effective refractive index; and Λ represents the grating period. A working principle diagram of FBG is shown in Fig. 2. If FBG is subject to force and temperature variations, those variations will affect the grating period, and the changes to the Bragg wavelength will be measured and retrieved from the coupler. Therefore, the reflected light spectrum of FBG plays a role in terms of allowing for physical quantity measurements through the monitoring of the FBG wavelength.

C. Impact Design

1) COMSOL Simulation: Regarding the exertion of external forces on outdoor cabinets in this experiment and because costly cabinets could not withstand frequent impact tests, this study adopted COMSOL Multiphysics software to perform simulations, mainly based on cost considerations. At first, a 3D outdoor cabinet was created using Solidworks, and this was then exported to COMSOL. Through COMSOL, stress was applied to the four sides of the cabinet in order to pinpoint the location for each side where the maximum strain would be perceived. Figure 2 shows the modal of the mass impact test of the outdoor optical fiber cabinets and the surface bonding location of the FBG sensor.

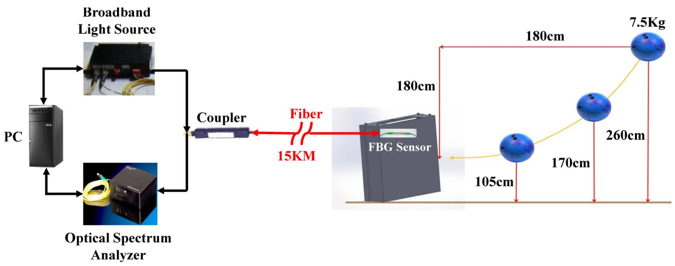

Fig. 3. The schematics of the mass impact test using a ball.

2) Mass Impact Tests (Bowling Ball): Fig. 3 presents the schematics of the mass impact test using a bowling ball. Before creating an impact alarm warning for the outdoor cabinet sensor system, the associated thresholds must be given. To identify the force of an impact that could possibly cause cabinet deformation, an impact procedure was designed using a commercially available bowling ball with a mass of 7.5 kg, to which two sleeve anchors were installed on two opposite sides of the ball; ropes of equal length were pulled through the two rings and fastened to a ceiling more than two meters above the ground, suspending the ball from the ceiling. Subsequently, the elevation of the ball above the ground was adjusted according to the simulated weakest point of the cabinet (Fig. 3).

In the tests, the ball was adjusted to the heights of 105 cm, 170 cm, and 260 cm, and then was released to impact against the cabinet with a free-fall pendulum motion. Disregarding the friction and windage and according to the law of conservation of energy, impact intensity can be measured by calculating the ball's velocity at the lowest point, i.e., its instantaneous velocity before striking the cabinet.

$$\frac{1}{2}mV_o^2 + mgh_o = \frac{1}{2}mV^2 + mgh \tag{2}$$

where Vo and V represent the initial velocity (= 0) and final velocity, respectively; h_o and h denote the ball height before the fall and the height of the impact point after the fall, respectively; and m is the mass of the ball. The final velocity V and the acceleration a are calculated as follows:

$$\mathrm{V} = \sqrt{2g(h_0 - \mathrm{h})} \tag{3}$$

$$a = \frac{V}{\Delta t}. \tag{4}$$

The impact force was obtained using Newton's second law of motion.

$$F = ma. \tag{5}$$

The measured impact duration was approximately 0.15 s according to the data obtained using an I-MON E-USB 2.0 spectrum analyzer (resolution = 0.001644 s). Therefore, the ball's impact forces on the cabinet were determined to be 108.75 N, 195.5 N, and 297 N at the heights of 105 cm, 170 cm, and 260 cm, respectively.

3) Roadside Impact Tests: In reality, most outdoor cabinets are installed on roadsides or pavements, rendering them prone to damage from traffic vehicles and vandalism. The roadside impact tests in this section were intended to simulate a variety of potential impacts (specifically, impacts from kicking, hammering, being struck by a motorbike, and being struck by a truck). Through observing the deviations of FBG wavelengths after the cabinet was hit, the impact alarm function was determined, and we sought to ensure that the outdoor cabinet sensor system was capable of identifying the prescribed impact conditions.

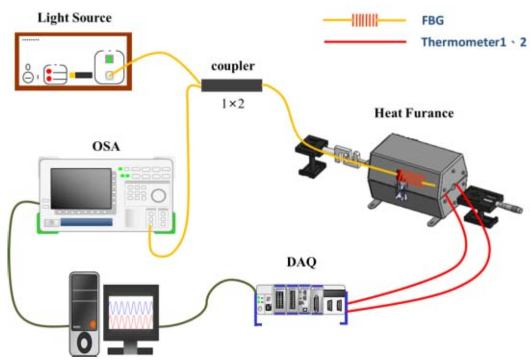

Fig. 4. Equipment arrangement in the temperature calibration test.

D. Temperature Calibration Tests

Fig. 4 illustrates the arrangement of optical equipment used in the temperature calibration tests: an oven, a heater, a broadband light source, a spectrum analyzer, and the FBG sensors. These optical fibers were fastened with tape. Two additional thermocouple devices were utilized for temperature references in this experiment, and the three thermometers were placed adjacent to each other to reduce measurement errors. After properly setting up all the equipment, the oven was switched on and the heater was activated, heating the oven from room temperature to 40 °C, 60 °C, 80 °C, and 100 °C in the respective tests, the readings on the thermocouple devices and the FBG reflective wavelengths on the spectrum analyzer were retrieved once every 60 s to generate the temperature variation and temperature-wavelength variation curves.

E. Monitoring System Design

Following the design process shown in Fig. 5, a real-time FBG monitoring system is created to monitor temperature and impacts to the cabinet. We utilize two FBG sensors for environmental monitoring of outdoor optical fiber cabinets. In order to overcome the effects of cross sensitivity of an FBG to strain and temperature, we use two FBG sensors, one for the strain with temperature cross effect, and the other one only for the temperature sensing (strain-free for temperature compensation, without surface bonding). By comparison these two FBGs, the temperature and strain variation can be monitored simultaneously. $\lambda 1$ and $\lambda 2$ refer to wavelengths corresponding to the combined strain-temperature effect and to temperature variation alone, respectively. The maximum wavelength changes caused by the temperature and impact strain variations of the cabinet were about 0.2 nm and 0.08nm, respectively. Therefore, the alarm thresholds of the $\lambda 1$ and $\lambda 2$ values were set to 0.2 nm and 0.08 nm.

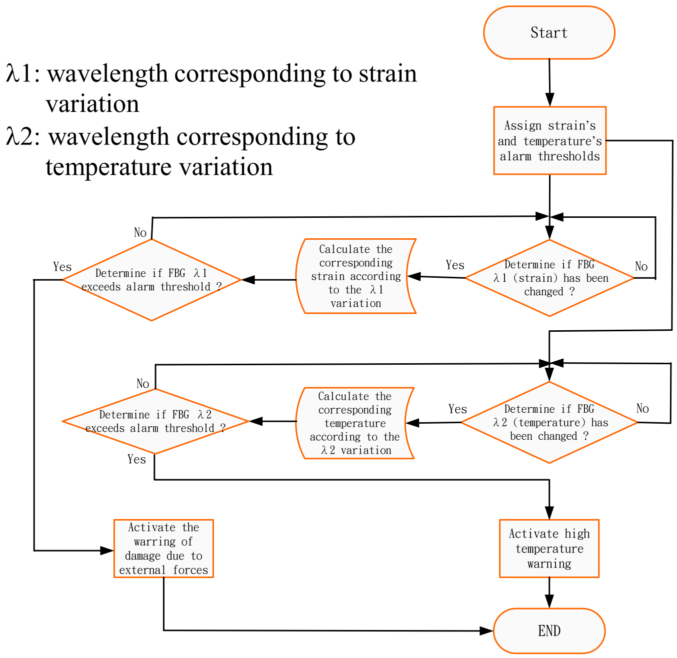

Fig. 5. The flow chart of the FBG monitoring system.

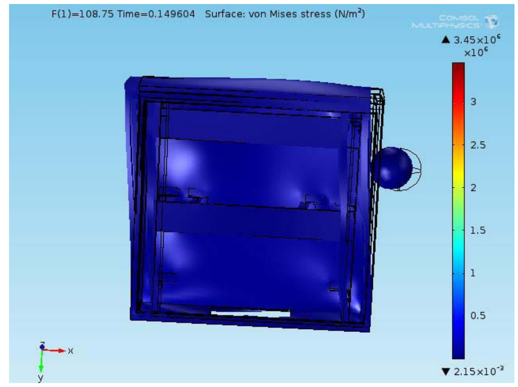

Fig. 6. Simulating impacts on a cabinet's side door.

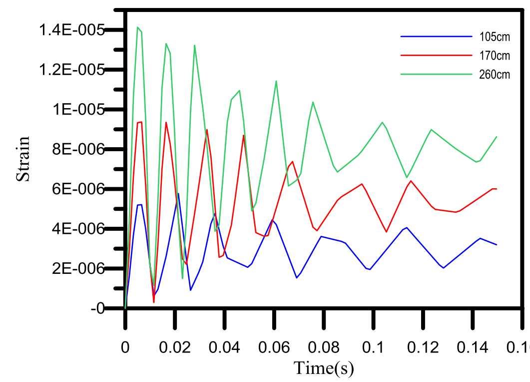

Fig. 7. Impact simulation results for three different heights.

The optical fibers in the cabinets had at least four cores (two were trunk lines and the other two were for backup). The packaged FBGs were attached to the center of the inner-top plane of an outdoor cabinet, and one of the backup optical fibers was adopted as the transmission channel. Next, the broadband light source and I-MON interrogation monitor (I-MON E-USB, Ibsen corp., Denmark) were placed at the telecommunication networks monitoring center and connected to the outdoor cabinets using patch cords in the user-end fiber optical distribution boxes for the purpose of remote monitoring.

III. Results and Discussion

A. COMSOL Simulation Results of Mass Impact Tests

The COMSOL simulation results were analyzed and discussed, and the temperature and impact tests were conducted in the laboratory to obtain the FBGs' wavelength deviation values. In effect, a 24-hour monitoring of the outdoor cabinet was conducted to verify the monitoring capabilities of the proposed outdoor cabinet monitoring system, which was developed using LabVIEW software. According to the observations of patrol officers, casual roadside impacts usually occur on a cabinet's side doors, causing deformation. Minor impacts may also destroy airtightness, allowing dust, biogas, or microorganisms to enter the cabinet. Severe impacts typically damage cabinet doors on rainy days, and may result in the complete destruction of expensive network equipment in the cabinets because of water seepage. Therefore, as illustrated in Fig. 6, impacts were applied to the side door in the simulation.

The simulation results shows that when equal amounts of force were applied to different spots on the cabinet door, the central spot incurred the largest deformation, indicating that the center was most vulnerable to external impacts that could, in turn, cause door deformation and air leakage. Consequently, this spot was adopted for conducting segmented impact tests and observing the extent of deformation; the critical value at which the impact detection alarm is activated was thereafter defined. Fig. 7 describes the simulation results of generating impacts on the cabinet door from three different heights.

B. Results of Mass Impact Tests

The impacts on the cabinet caused by the ball falling from heights of 105 cm, 170 cm, and 260 cm above the ground were 108.75 N, 195.5 N, and 297 N, respectively. Fig. 8 illustrates the FBG test results, which were compared with the strain variation results measured at the moments of impact (Fig. 9).

The impacts generated by the ball falling from the heights of 105 cm and 170 cm caused no substantial damage or dents to the cabinet door. However, the impact created by the ball falling from 260 cm caused a significant dent to the cabinet door. The results show that the door latch was flipped open and that the hinges creaked when the door was opened and closed. The maximum amplitude of the largest impact was recorded by the spectrum analyzer as $\Delta\lambda_{max} = 0.012847$ nm, which can serve as the critical reference value or threshold for the impact alarm function in the outdoor cabinet monitoring system.

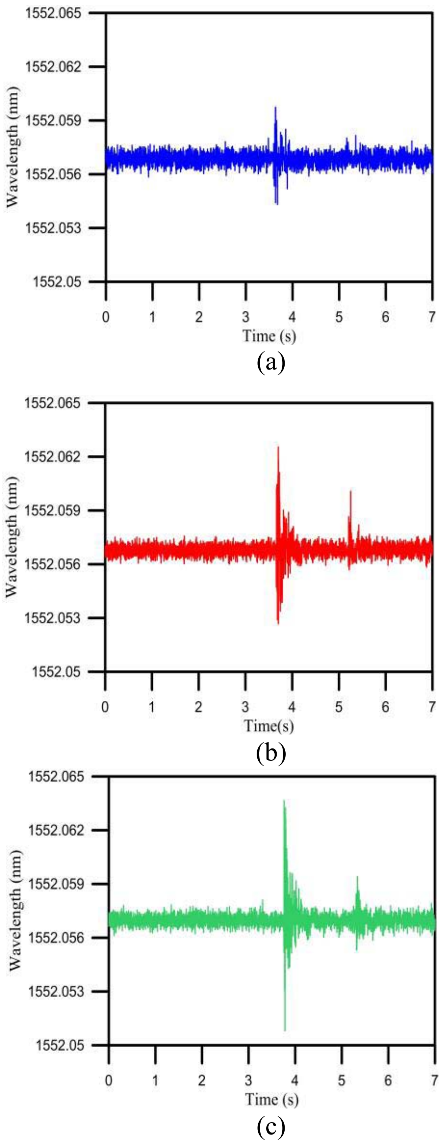

Fig. 8. Relationship between wavelengths and impact time durations due to the bowling ball. (a) Impact of 108.75 N. (b) Impact of 195.5 N. (c) Impact of 297 N.

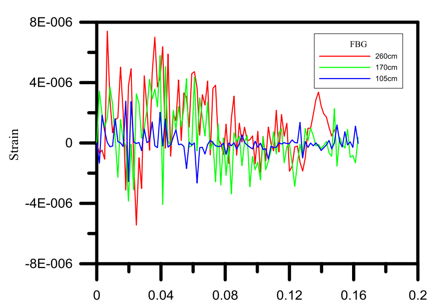

Fig. 9. Strain variations associated with impacts from different heights.

C. Comparing the Actual Tests With the Simulated Tests

The results of the actual and simulated tests indicated that when the ball hit the outdoor cabinet, the deviation of the strain was small. When the ball hit the door from the height of 105 cm, the maximum deviation was 0.002766 at 0.018084 s, and when the ball hit from the heights of 170 cm and 260 cm, the maximum shifts were 0.002397 at 0.037812 s and 0.0074 at 0.006576 s, respectively (Fig. 10).

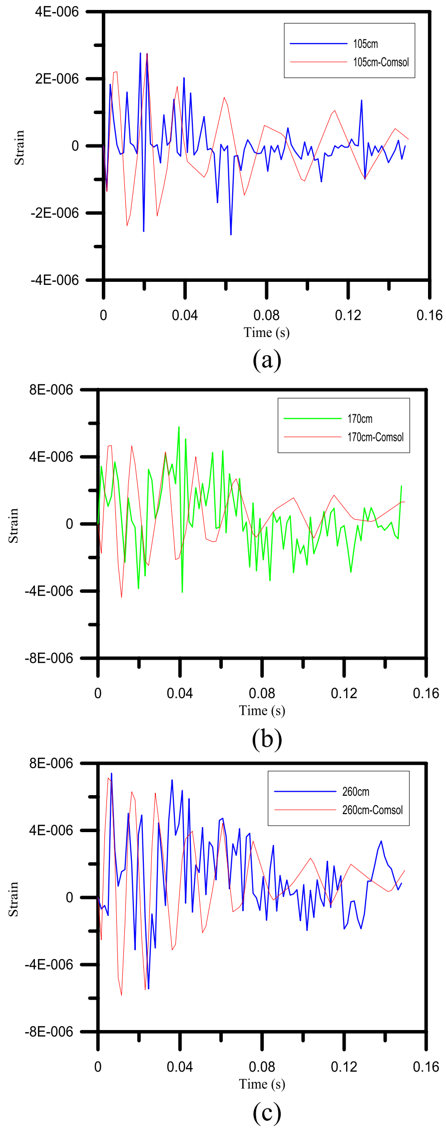

Fig. 10. Comparing the actual impacts created by the falling ball with the simulated impacts. (a) 105 cm. (b) 170 cm. (c) 260 cm.

D. Results of Roadside Impact Simulation

The wavelength changes due to the impacts on the cabinet from kicking, hammering, a 150-cc motorbike, and a truck were recorded in the FBG sensor (Fig. 11). The results indicated that those different scenarios and their corresponding durations of impacts yielded distinct responses from the sensor. Intuitively, the impact intensity of a causal kick, which had a maximum wavelength variation of $\Delta\lambda \max = 0.005409$ nm, was not sufficient to damage the cabinet. The impacts from hammering ($\Delta\lambda\max = 0.050456$ nm), a 150-cc motorbike ($\Delta\lambda \max = 0.035585$ nm), and a truck ($\Delta\lambda\max = 0.053290$ nm), however, were absolutely sufficient to damage the structure of the cabinet door. Among these impact sources, the truck caused the most severe damage to the cabinet, resulting in the deformation and malfunction of the cabinet

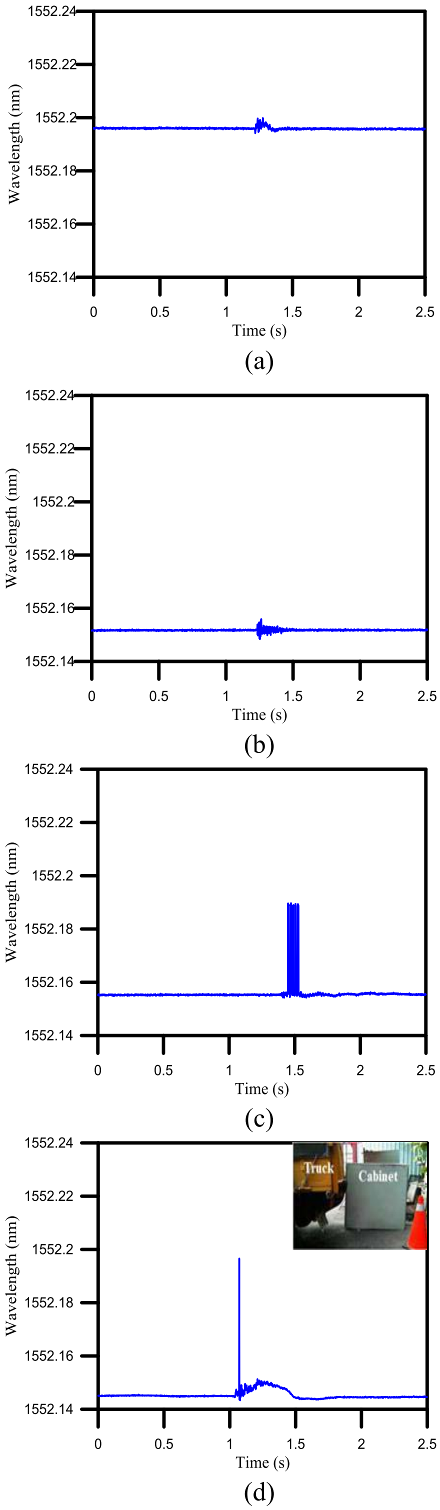

Fig. 11. Results of roadside impact tests. (a) Kicking. (b) Hammering. (c) 150-cc motorbike. (d) Truck.

door. However, the maximum amplitude of the truck ($\Delta\lambda_{\max} = 0.053290$ nm) measured by the FBG sensor was similar to that caused by hammering. This unexpected result was attributed to the excessive impact generated by the truck, which uprooted the four nails affixed to the bottom of the cabinet and thus allowed the dispersal of the force.

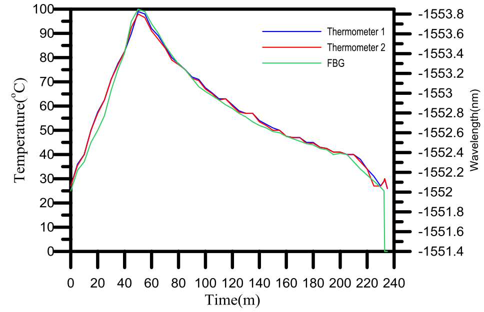

Fig. 12. Temperature variations of the FBG sensor and the two thermocouple devices.

E. Temperature Tests

To verify the temperature sensing capabilities of the FBG sensors, a data acquisition (DAQ) device from National Instruments was employed to obtain the temperature data measured by the two thermocouple devices. The temperature variation curves of the FBGs and the two thermocouple devices were recorded and are shown in Fig. 12, in which the blue and red curves represent the temperature increases in the thermocouple devices recorded using a DAQ device on a minute-by-minute basis, and the green curve indicates the readings of the FBGs. The results show that the FBG sensors accurately measured temperature increases during the three periods of 19–23, 25–38, and 49–53 minutes, whereas the thermometers continued to exhibit temperature increases during these three durations. This was caused by the insensitivity and instability of the thermocouples with respect to temperature. As a matter of fact, the FBG sensors possess a superior linear relationship to temperature variation.

After the FBG temperature test, the relationship between the five holding temperature points (25 °C, 40 °C, 60 °C, 80 °C, and 100 °C) and the optical fiber wavelength deviation was determined; the relationship is illustrated in Fig. 13, in which a near-linear relationship between temperature and wavelength deviation can be observed.

Based on Fig. 13, an approximated linear equation can be derived through linear regression analysis: $y = 1551.41202 + 0.02303x$, where 0.02303 represents the FBG temperature sensitivity coefficient K_T (FBG wavelength deviated by 0.02303 nm for every 1 °C temperature increase). This equation can be employed to serve as the conversion equation of temperature vs. wavelength deviation for the outdoor cabinet monitoring system.

F. Results of Actual Tests on Outdoor Cabinets

Following the test structure in Fig. 2, a 24-hr. temperature monitoring test was conducted, and the results are shown in Fig. 14. The maximum temperature, 70 °C, Occurred around 14:00. Additionally, a hammer was used to simulate different levels of impacts. When the impact exceeded the designated critical value, the monitoring system emitted a red light on the screen and warning sounds as a reminder to the supervisor, while also automatically recording wavelength variations four seconds prior to and after the incident in a log file for future reference.

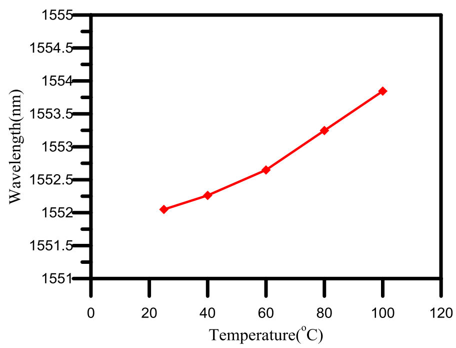

Fig. 13. Relationship between temperature and FBG wavelength.

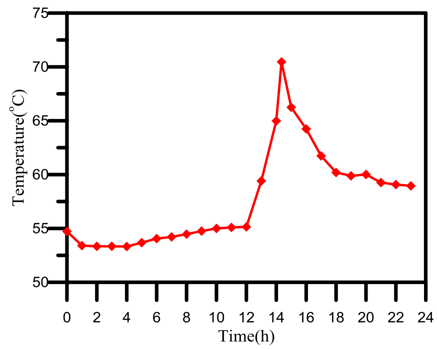

Fig. 14. Results of the 24-hr. temperature monitoring of an outdoor cabinet.

IV. Conclusion

This study developed a real-time monitoring system for outdoor cabinet temperatures and impacts by obtaining temperature coefficients and data on critical impact wavelength deviations in a series of experiments. A monitoring system was devised based on the collected data using LabVIEW. The results of experiments and actual tests are summarized as follows.

1) The system can instantly monitor temperature changes and impacts affecting outdoor cabinets and telecommunications equipment, providing instant knowledge of network status to improve internet stability and service quality.
2) The temperature tests prove the existence of an excellent linear relationship between the central wavelength shifts of FBG with respect to temperature. The sensitivity of the FBG sensor in this study was 0.02303 nm/°C. However, FBGs should be firmly secured at an appropriate location to reduce inaccuracy in sensor measurements during monitoring processes.
3) The main structure of the outdoor cabinet is simple and therefore allows complete transmission of an impact vibration to the FBGs on the top of the cabinet. Impact tests showed that a force of over 297 N on a single spot caused door deformation, and that a deviation of over 0.05 nm can also cause door deformation.
4) During the actual monitoring of the outdoor cabinet through a telecommunication networks monitoring center, almost no insertion loss occurred in the FBG wires in the laboratory. However, the length of the optical fiber between TSPs and outdoor cabinets may range from 10 to 20 km. Therefore, to improve the accuracy of the monitoring system, the 2.5–5 dBm attenuation of a broadband light source must be accounted for when executing the monitoring programs.

Applications of FBGs to various fields have increased in recent years. In addition to the applications described in this study and the proposed environmental monitoring of outdoor cabinets, other potential applications of FBGs to elements of telecom network infrastructure (e.g., in fibers connected to homes, in residential security monitoring and in the monitoring of wireless base stations in remote areas) may be realized in the near future.

References

[1] G. Xiao, N. Mrad, F. Wu, Z. Zhang, and F. Sun, "Miniaturized optical fiber sensor interrogation system employing echelle diffractive gratings demultiplexer for potential aerospace applications," *IEEE Sensors J.*, vol. 8, no. 7, pp. 1202–1207, Jul. 2008.

[2] H. F. Lima *et al.*, "Structural health monitoring of the church of Santa Casa da MisericÓrdia of Aveiro using FBG sensors," *IEEE Sensors J.*, vol. 8, no. 7, pp. 1236–1242, Jul. 2008.

[3] T. Guo, B. Liu, H. Zhang, Q. Zhao, and X. Dong, "Linear and Gaussian chirped fiber Bragg grating and its applications in fiber-optic filtering and sensing systems," *IEEE Photon. Technol. Lett.*, vol. 19, no. 14, pp. 1096–1098, Jul. 15, 2007.

[4] A. Grillet *et al.*, "Optical fiber sensors embedded into medical textiles for healthcare monitoring," *IEEE Sensors J.*, vol. 8, no. 7, pp. 1215–1222, Jul. 2008.

[5] M. L. Filograno *et al.*, "Real-time monitoring of railway traffic using fiber Bragg grating sensors," *IEEE Sensors J.*, vol. 12, no. 1, pp. 85–92, Jan. 2012.

[6] J. Luo, Y. Hao, Q. Ye, Y. Hao, and L. Li, "Development of optical fiber sensors based on Brillouin scattering and FBG for on-line monitoring in overhead transmission lines," *J. Lightw. Technol.*, vol. 31, no. 10, pp. 1559–1565, May 15, 2013.

[7] K. O. Hill, B. Malo, F. Bilodeau, D. C. Johnson, and J. Albert, "Bragg gratings fabricated in monomode photosensitive optical fiber by UV exposure through a phase mask," *Appl. Phys. Lett.*, vol. 62, no. 10, pp. 1035–1037, 1993.

[8] A. F. da Silva, A. F. Gonçalves, L. A. de Almeida Ferreira, F. M. M. Araújo, P. M. Mendes, and J. H. Correia, "PVC smart sensing foil for advanced strain measurements," *IEEE Sensors J.*, vol. 10, no. 6, pp. 1149–1155, Jun. 2010.

[9] A. F. da Silva, A. F. Gonçalves, P. M. Mendes, and J. H. Correia, "FBG sensing glove for monitoring hand posture," *IEEE Sensors J.*, vol. 11, no. 10, pp. 2442–2448, Oct. 2011.

[10] R. P. Rocha, A. F. da Silva, J. P. Carmo, and J. H. Correia, "FBG in PVC foils for monitoring the knee joint movement during the rehabilitation process," in *Proc. Int. Conf. IEEE Eng. Med. Biol. Soc.*, Aug./Sep. 2011, pp. 458–461.

[11] G. Wild, "Optical fiber Bragg grating sensors applied to gas turbine engine instrumentation and monitoring," in *Proc. IEEE Sensors Appl. Symp. (SAS)*, Feb. 2013, pp. 188–192.

[12] S. N. M. Ghazali, N. A. M. Yahya, and S. Sulaiman, "Characterization of fiber Bragg grating as optical temperature sensor for pipeline water leakage inspection," in *Proc. IEEE 3rd Int. Conf. Syst. Eng. Technol. (ICSET)*, Aug. 2013, pp. 173–177.

[13] D. Barrera, V. Finazzi, J. Villatoro, S. Sales, and V. Pruneri, "Packaged optical sensors based on regenerated fiber Bragg gratings for high temperature applications," *IEEE Sensors J.*, vol. 12, no. 1, pp. 107–112, Jan. 2012.

[14] M. Liu, Z. Zhou, X. Tao, and Y. Tan, "A dynamometer design and analysis for measurement the cutting forces on turning based on optical fiber Bragg grating sensor," in *Proc. 10th World Congr. Intell. Control Autom.*, Jul. 2012, pp. 4287–4290.

[15] Q. Yu, Y. Zhang, Y. Dong, Y. P. Li, C. Wang, and H. Chen, "Study on optical fiber Bragg grating temperature sensors for human body temperature monitoring," in *Proc. Symp. Photon. Optoelectron. (SOPO)*, May 2012, pp. 1–4.

[16] K. Hung, C. C. Lee, W. M. Chen, S.-O. Choy, and P. Kwok, "Development of novel wearable sensors for mobile health," in *Proc. IEEE-EMBS Int. Conf. Biomed. Health Informat.*, Jan. 2012, pp. 745–747.
[17] K. M. Sousa *et al.*, "Optical fiber Bragg grating sensors applied on energy conversion systems," in *Proc. Microw. Optoelectron. Conf. (IMOC)*, Aug. 2013, pp. 1–5.
[18] D. H. Wang, S. S. H. Hwang, S. A. Maunder, N. G. Blenman, and J. W. Arkwright, "Optical fiber Bragg grating based chemical sensor," in *Proc. IEEE Sensors*, Oct. 2012, pp. 1–3.
[19] G. Allwood, S. Hinckley, and G. Wild, "Optical fiber Bragg grating based intrusion detection systems for homeland security," in *Proc. IEEE Sensors Appl. Symp. (SAS)*, Feb. 2013, pp. 66–70.
[20] C. S. Park, K. I. Joo, S. W. Kang, and H. R. Kilm, "A PDMS-coated optical fiber Bragg grating sensor for enhancing temperature sensitivity," *J. Opt. Soc. Korea*, vol. 15, no. 4, pp. 329–334, 2011.

Wen-Ping Chen received the B.S. degree from the National Taiwan Institute of Technology, Taipei, Taiwan, in 1992, the M.S. degree from National Sun Yat-sen University, Kaohsiung, Taiwan, in 2000, and the Ph.D. degree from the National Kaohsiung University of Applied Sciences, Kaohsiung, in 2008, all in electrical engineering. He is an Associate Professor of Electrical Engineering with the National Kaohsiung University of Applied Sciences. His current research interests include the application of Internet of things and protocol design of optical networks.

Fu-Hung Shih received the B.S. degree in electronic engineering from the National Yunlin Institute of Technology, Yunlin, Taiwan, in 1994, and the M.S. degree in electrical engineering from the National Kaohsiung University of Applied Sciences, Kaohsiung, Taiwan, in 2008. He is an Associate Manager of private network company. His research focuses on optical networks protection and network architecture management.

Po-Jun Tseng received the B.S. degree in electrical engineering from Cheng Shiu University, Kaohsiung, Taiwan, in 2005, the M.S. degree in electrical engineering from the National Kaohsiung University of Applied Sciences, Kaohsiung, in 2013. He was with Chunghwa Telecom Company, Ltd., Taipei, Taiwan, as an Engineer. His expertise is in the telecommunications line maintenance.

Chih-Hsien Shao received the B.S. degree from the Department of Mechanical Engineering, Kaohsiung University of Applied Sciences, Kaohsiung, in 2012, where he is currently pursuing the master's degree at the Department of Mechanical Engineering. His research interests include fiber-optic sensors and microelectromechanical systems.

Chia-Chin Chiang received the B.S. and M.S. degrees from the Department of Mechanical and Mechatronic Engineering, National Taiwan Ocean University, Keelung, Taiwan, in 1998 and 2000, respectively, and the Ph.D. degree from National Taiwan University, Taipei, Taiwan, in 2005. He became an Assistant Professor with the Department of Mechanical Engineering, Kaohsiung University of Applied Sciences, Kaohsiung, Taiwan, in 2006, and an Associate Professor in 2011. His research interests include fiber Bragg gratings, optical fiber sensors, and smart materials and structures.